Experimental subwavelength localization of scatterers by decomposition of the time reversal operator interpreted as a covariance matrix

Claire Prada[a] and Jean-Louis Thomas
Laboratoire Ondes et Acoustique, Université Denis Diderot, UMR CNRS 7587, ESPCI, 10 rue Vauquelin, 75231 Paris Cedex 05, France

(Received 20 May 2002; revised 19 February 2003; accepted 19 February 2003)

The D.O.R.T. method (French acronym for Decomposition of the Time Reversal Operator) is an active remote sensing technique using arrays of antennas for the detection and localization of scatterers [Prada *et al.*, J. Acoust. Soc. Am. **99**, 2067–2076 (1996)]. The analogy between the time reversal operator and the covariance matrix used for classical sources separation in passive remote sensing [Bienvenu *et al.*, IEEE Trans. ASSP **31**, 1235–1247 (1983)] is established. Then, an experiment of subwavelength detection and localization of point-like scatterers with a linear array of transducers is presented. Using classical estimators in reception like Maximum-Likelihood and Multiple Signal Characterization (MUSIC), two point-like scatterers separated by $\lambda/3$ and placed at 100λ from the array of transducers are resolved. In these experiments, the role of multiple scattering and the existence of additional eigenvectors associated with dipolar and monopolar radiation of each scatterer is discussed. © *2003 Acoustical Society of America.* [DOI: 10.1121/1.1568759]

PACS numbers: 43.60.Pt, 43.28.We, 43.20.Fn [JCB]

I. INTRODUCTION

Remote sensing techniques are developed for many applications in the field of electromagnetic or acoustic waves. Methods with superresolution properties, like MUSIC, have been the subject of an intense field of research in the framework of passive array processing. However, numerous applications involve the detection and the localization of scatterers and consequently require array processing adapted to active array, like the D.O.R.T. method described below. In this work we establish the analytical link between D.O.R.T. and methods developed for the passive detection of sources that are based on an eigendecomposition of a covariance matrix. This formal demonstration is illustrated by an experiment in which subwavelength resolution is obtained.

Active transducer arrays with electronic focusing and steering capabilities are now commonly used in medical imaging; they have also become available for nondestructive evaluation and even in underwater acoustics. In the Laboratoire Ondes et Acoustique, a new adaptive detection technique, the D.O.R.T. method was implemented to optimize the use of such arrays. The D.O.R.T. method (a French acronym for ''Décomposition de l'Opérateur de Retournement Temporel) is an active detection technique that efficiently detects and separates the responses of several scatterers in homogeneous or heterogeneous media,[1–3] even in the presence of reverberation.[4,5] It was applied to the detection of flaws in nondestructive testing,[6,7] target detection and identification in underwater acoustics, and in electromagnetism as the first stage in the resolution of an inverse problem.[8]

This method is based on the singular value decomposition of the matrix $\mathbf{K}(\omega)$ of the interelement responses of the array at frequency ω. The processing assumes only linearity and time shift invariance of the propagation. This decomposition provides the eigenvector decomposition of the product ${}^t\mathbf{K}^*(\omega)\mathbf{K}(\omega)$, the so-called time reversal operator. Hence, this processing, like time reversal or phase conjugation, is adaptive to phase aberrations induced by heterogeneities in the medium. It was shown that when the scatterers are small compared to the wavelength, the number of significant singular values is, in general, equal to the number of scatterers. Furthermore, for well-resolved scatterers of distinct apparent reflectivities, the associated singular vector is the response of one scatterer to the array. In fact, Chambers[11] has shown analytically that for a point-like scatterer, there are four singular values (three for a 2-D configuration) of which three are very weak in most configurations. When the scatterers have sizes comparable to or larger than the wavelength, there is a whole set of singular values and singular vectors associated either with the specular part or with resonances of the scattered wave.[12]

In the field of source detection, sophisticated array signal processing was developed to estimate the number, direction, and signal intensity of sources. Among them, the signal subspace-type techniques were given great attention. Such methods start with an estimate of the data covariance matrix deduced from the impinging wavefront on the receiving array. For noncorrelated sources, the decomposition of this matrix into a source space and a noise space provides the number of sources. Then, their directions and strengths are obtained by various estimators applied to the source space. These processings are employed either in RADAR and SONAR for the detection and separation of sources.[13,14]

In a first stage, the connection between the D.O.R.T. method and classical array processing is established by identifying the scatterers with secondary sources and showing that the time reversal operator can be written as a covariance matrix like the one introduced in passive source detection. In

[a]Electronic mail: claire.prada-julia@espci.fr

a second stage, classical estimators in reception like Maximum-Likelihood (ML) and MUltiple SIgnal Characterization (MUSIC), will be applied in order to evaluate the resolving power of this active method. The possibility of applying MUSIC processing in reception was shown independently by Devaney[15] and also discussed by Cheney.[16]

A 2-D experiment with a linear array and two identical wires ten times thinner than the wavelength will illustrate the resolution and the precision of the method in the presence of noise. It will be shown that the method can separate and locate two scatterers positioned less than half a wavelength apart. Furthermore, this will give an experimental evidence that each target is associated with a 3-D signal space, as predicted by Chambers, and will also illustrate how multiple scattering affects the singular values distribution for close scatterers.

II. THE D.O.R.T. METHOD

To recall the D.O.R.T. method in a general manner, a propagating medium with point-like scatterers is considered. The medium may be heterogeneous with gradual variation of density and sound speed. An array of M transmitters and an array of L receivers are used to detect these scatterers. Assuming time shift invariance and linearity, any transmit–receive process performed from array #1 of M transmitters to array #2 of L receivers, is described by the $L\times M$ inter-element impulse responses $k_{lm}(t)$. The expression of $r_l(t)$, the signal received on element number l, is the following:

$$r_l(t)=\sum_{m=1}^{M} k_{lm}(t)\otimes e_m(t)+b_l(t), \tag{1}$$

where $e_m(t)$ is the signal applied to element number m and $b_l(t)$ is noise. A Fourier transform of Eq. (1) leads to

$$R(\omega)=\mathbf{K}(\omega)E(\omega)+B(\omega), \tag{2}$$

where $R(\omega)$ is the received vector signal, $\mathbf{K}(\omega)$ is the transfer matrix from transmit array to receive array, $E(\omega)$ is the emitted vector and $B(\omega)$ a noise vector.

The transfer matrix $\mathbf{K}(\omega)$ can be measured by transmitting successively a set of N independent vectors. The Singular Value Decomposition (SVD) of this complex matrix is

$$\mathbf{K}(\omega)=\mathbf{U}(\omega)\Sigma(\omega)^t\mathbf{V}^*(\omega), \tag{3}$$

where $\Sigma(\omega)$ is a real diagonal matrix of singular values, $\mathbf{U}(\omega)$ and $\mathbf{V}(\omega)$ are unitary matrices.

The physical meaning of this singular value decomposition is illuminated through the analysis of the iterative time reversal process. This process has been widely described[1–3] for a single array of transmit and receive transducers and generalized to separate arrays[4] and the time reversal operator was defined in a general manner as ${}^t\mathbf{K}^*(\omega)\mathbf{K}(\omega)$. Once the matrix $\mathbf{K}(\omega)$ is measured, the processing is purely numerical so that the role of the two arrays may be switched. At this stage, only the reciprocity principle, the time shift invariance, and the linearity of the medium are used. The SVD of $\mathbf{K}(\omega)$ can now be interpreted: the eigenvalues of ${}^t\mathbf{K}^*(\omega)\mathbf{K}(\omega)$ are the squares of the singular values of $\mathbf{K}(\omega)$ and its eigenvectors are the columns of $\mathbf{V}(\omega)$. In consequence, the singular vectors of $\mathbf{K}(\omega)$ are the invariants of the iterative time reversal process. These invariants are quite well known for ''Rayleigh''-type scatterers and single scattering. In this case, the transfer matrix $\mathbf{K}(\omega)$ is the product of three matrices, $\mathbf{H}_2(\omega)$, $\mathbf{D}(\omega)$, and $\mathbf{H}_1(\omega)$, respectively, modeling (1) the propagation from the transmit array toward the scatterers, (2) the scattering, and (3) the propagation from the scatterers toward the receive array:

$$\mathbf{K}(\omega)=\mathbf{H}_1(\omega)\mathbf{D}(\omega)\mathbf{H}_2(\omega). \tag{4}$$

From this equation, one can see that the rank of the transfer matrix is less than or equal to the number of scatterers. If multiple scattering is negligible then $\mathbf{D}(\omega)$ is a diagonal matrix. Furthermore, if the scatterers have distinct reflectivities and are ideally resolved by both transmit and receive arrays, then there is a one-to-one correspondence between the scatterers and the singular vectors. In other words, each vector corresponds to the response of one scatterer to the array.

In fact, the assumption of isotropic scattering is only true for a point-like discontinuity in compressibility. In general, a scatterer is also associated with a density variation and a recent study[11] has shown that four eigenvalues of the time reversal operator are associated with each scatterer. However, for hard materials, if the scatterer is much smaller than a wavelength, then three of the eigenvalues are much smaller than the dominant one. This is why the multiple eigenstates have not been observed in experiments to date.

Following Eq. (4), the time reversal operator is now written as

$${}^t\mathbf{K}^*(\omega)\mathbf{K}(\omega)={}^t\mathbf{H}_2^*(\omega)\mathbf{D}^*(\omega){}^t\mathbf{H}_1^*(\omega)\mathbf{H}_1(\omega)\mathbf{D}(\omega)\mathbf{H}_2(\omega). \tag{5}$$

We will see below how this operator can be considered as an estimate of a covariance matrix of the kind introduced in passive source detection.

III. THE COVARIANCE MATRIX AND THE TIME REVERSAL OPERATOR

Before discussing the analogy between the time reversal operator and the covariance matrix, the construction of the covariant matrix in passive source detection is recalled.

A. The covariance matrix for passive source detection technique

In usual descriptions of source detection techniques, a distribution of unknown sources and an array of receivers are considered.[9,10] The problem to be solved is to find the number of sources and their directions.

Let $(s_1(t),\ldots,s_d(t))$ be the signals emitted by d unknown sources, and let $(r_1(t),\ldots,r_L(t))$ be the signals measured on an array of L receivers. Assuming that the propagation is linear and time invariant, the signal measured on receiver number l can be written as

$$r_l(t)=\sum_i h_{li}(t)\otimes s_i(t)+b(t), \tag{6}$$

where, for $1\leqslant i\leqslant d$ and $1\leqslant l\leqslant L$, $h_{li}(t)$ is the response from source number i to receiver number l. In the frequency domain, Eq. (6) can be written in matrix form as

$$R(\omega)=\mathbf{H}(\omega)S(\omega)+B(\omega), \tag{7}$$

where $R(\omega)$ is the receive vector signal, $\mathbf{H}(\omega)$ is the transfer matrix from the source onto the array, $S(\omega)$ is the source vector, and $B(\omega)$ the noise vector. If M realizations of the receive vector are measured $[R_m(\omega),1\leqslant m\leqslant M]$, an estimate of the covariance matrix can be obtained by averaging of the corresponding matrices $\mathbf{C}_m(\omega)=R_m(\omega)^t R_m(\omega)^*$.

Assuming that the medium and source positions are time invariant and that the noise is not correlated to the sources, the covariance matrix is expressed from the source covariance matrix as

$$\langle \mathbf{C}(\omega)\rangle=\mathbf{H}(\omega)\langle S(\omega)\,{}^tS(\omega)^*\rangle\,{}^t\mathbf{H}(\omega)^* + \langle B(\omega)\,{}^tB(\omega)^*\rangle. \tag{8}$$

If the sources are uncorrelated, the matrix $\langle S(\omega)\,{}^tS(\omega)^*\rangle$ is diagonal. If the elements of the noise vector $B(\omega)$ are also uncorrelated, mean zero and variance σ, then the noise term is

$$\langle B(\omega)\,{}^tB(\omega)^*\rangle=\sigma^2\mathbf{I}. \tag{9}$$

The next stage of spectral methods is to compute an eigendecomposition of the covariance matrix $\langle \mathbf{C}(\omega)\rangle$. If the responses from the sources are orthogonal vectors, then the preceding expression provides the diagonalization of the covariance matrix. The eigenvalues are the following:

$$\lambda_i=\langle |S_i(\omega)|^2\rangle\sum_{l=1}^{L}|H_{il}(\omega)|^2+\sigma^2. \tag{10}$$

The eigenvalues are proportional to the average intensity of the sources and the eigenvectors are the vectors H_i, i.e., the frequency response from the source to the array. However, in a general case, the responses from the sources to the array are not orthogonal vectors.

B. Link between the time reversal operator and the covariance matrix

We now reconsider the measurement of the transfer matrix in a scattering experiment with ''Rayleigh-type'' scatterers. We use the same notations as in Eqs. (4) and (5).

Insonifying the medium with a pulse on transducer n, the received vector signal is the nth column of $\mathbf{K}$ and is expressed as

$$R_n(\omega)=\mathbf{H}_1(\omega)\mathbf{D}(\omega)H_{2n}(\omega)+B_n(\omega), \tag{11}$$

where $H_{2n}(\omega)$ is the nth column of $\mathbf{H}_2(\omega)$ and $B_n(\omega)$ is the noise vector.

The vector $\mathbf{D}(\omega)H_{2n}(\omega)$ can be considered as one realization of the source vector $S(\omega)$ of Eq. (7). The measurement of the N columns of $\mathbf{K}$ is analogous to N measurements of the source signal in passive detection (Sec. III A). If the aperture of the array and the number of elements are large enough, there will be enough diversity in the measurements to decorrelate these secondary sources.

Though the responses of the scatterers $R_n(\omega)$ are purely deterministic, they can be used to built a ''pseudocovariance matrix'' as follows:

$$\tilde{\mathbf{C}}(\omega)=\sum_n R_n(\omega)^t R_n^*(\omega). \tag{12}$$

Using the expression of $R_n(\omega)$ in Eq. (11), $\tilde{C}(\omega)$ is written as

$$\begin{aligned}\tilde{\mathbf{C}}(\omega)=&\mathbf{H}_1(\omega)\mathbf{D}(\omega)\\ &\times\left(\sum_n H_{2n}(\omega)^t H_{2n}^*(\omega)\right)\mathbf{D}^*(\omega)^t\mathbf{H}_1^*(\omega)\\ &+\mathbf{H}_1(\omega)\mathbf{D}(\omega)\left(\sum_n H_{2n}(\omega)^t B_n^*(\omega)\right)\\ &+\left(\sum_n B_n(\omega)^t H_{2n}^*(\omega)\right)\mathbf{D}^*(\omega)^t\mathbf{H}_1^*(\omega)\\ &+\left(\sum_n B_n(\omega)^t B_n^*(\omega)\right).\end{aligned} \tag{13}$$

If the noise vector is not correlated to the scatterer responses, and if the number of measurements is large enough, the cross-terms vanish. Using Eq. (9) the expression simplifies to

$$\tilde{\mathbf{C}}(\omega)\cong\mathbf{H}_1(\omega)\mathbf{D}(\omega)^t\mathbf{H}_2(\omega)\mathbf{H}_2^*(\omega)\mathbf{D}^*(\omega)^t\mathbf{H}_1^*(\omega) + n\sigma^2\mathbf{I}. \tag{14}$$

In the absence of noise ($\sigma=0$), this last expression is exactly the time reversal operator $\mathbf{K}(\omega)^t\mathbf{K}^*(\omega)$ [see Eq. (5)]. It can also be compared with Eq. (8), in which the source covariance matrix $\langle S(\omega)^tS(\omega)^*\rangle$ is replaced by the matrix $\Sigma_n\mathbf{D}(\omega)^tH_{2n}(\omega)H_{2n}^*(\omega)\mathbf{D}^*(\omega)=\mathbf{D}(\omega)^t\mathbf{H}_2(\omega)\mathbf{H}_2^*(\omega)\mathbf{D}^*(\omega)$, where the average is taken over the different emissions. In general, when the number of scatterers is less than the number of emitters, the rank of this last matrix is equal to the number of scatterers.

The next stage consists in computing the eigenvalues and eigenvectors of the covariance matrix, which is equivalent to computing an SVD of the transfer matrix $\mathbf{K}$. This decomposition is a way of sorting the data from most dominant to the weakest contribution.

IV. DETECTION PROCESSING AND SUPER-RESOLUTION

In order to improve the resolution of the D.O.R.T. method, we have tried two estimators developed in classical array processing using the covariance matrix: Maximum Likelihood (ML) and MUSIC. To perform this analysis the vector signal $G(M)$ received by the array from a scatterer located at point M has to be modeled. In our model we choose the Green's function for free space.

The Maximum Likelihood estimator looks for the maxima of the function $I_{\mathrm{ML}}(M)$:

$$I_{\mathrm{ML}}(M)=\frac{1}{{}^tG^*(M)\mathbf{C}^{-1}G(M)}. \tag{15}$$

As the inverse of the covariance matrix may be computed by using the SVD of $\mathbf{C}$, Eq. (15) becomes

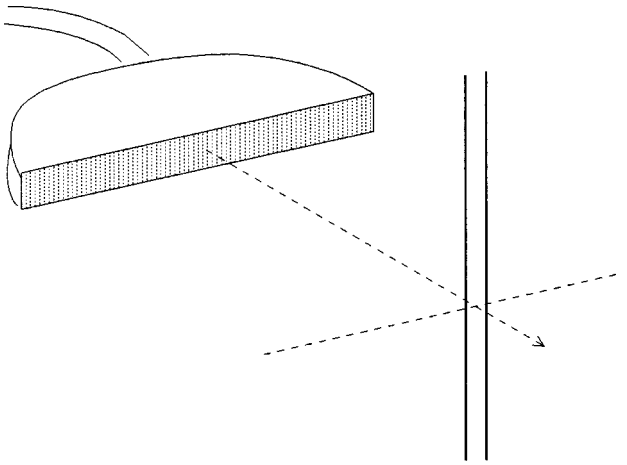

FIG. 1. Experimental setup.

$$I_{\mathrm{ML}}(M)=\frac{1}{{}^{t}G^{*}(M)\mathbf{U}\mathbf{\Lambda}^{-1}\,{}^{t}\mathbf{U}^{*}G(M)}$$

$$=\frac{1}{\sum_{i=1}^{L}\frac{1}{\lambda_i}|\langle\mathbf{U}_i|G(M)\rangle|^2}, \tag{16}$$

where $\Lambda=\Sigma\Sigma$ is the diagonal matrix composed of the eigenvalues of $C(\omega)$. A great advantage of this method is that it does not require the knowledge of the source space dimension.

If the dimension of the signal space, p, is known or can be estimated from the singular value distribution, then the MUSIC algorithm applies. The estimator is then

$$I_{\mathrm{MU}}(M)=\frac{1}{1-\Sigma_{i=1}^{p}|\langle\mathbf{U}_i|G(M)\rangle|^2}$$

$$=\frac{1}{\sum_{i=p+1}^{L}|\langle\mathbf{U}_i|G(M)\rangle|^2}. \tag{17}$$

This function is the inverse of the square of the Euclidean distance from the Green's vector $G(M)$ to the signal space. These two estimators are very similar, but MUSIC gives more importance to the eigenvector of the noise space.

It appears that these two estimators are nonlinear combinations of the back-propagation of each singular vector, $I_v(M)=|\langle\mathbf{V}|G(M)\rangle|$, used in our preceding papers.[3]

In all of these three methods, the choice of the Green's function is crucial and any *a priori* knowledge introduced to improve the model is worth trying.

V. EXPERIMENTAL RESULTS

The experimental results are obtained in a 2-D geometry with a linear transmit and receive array and two point-like scatterers (Fig. 1). A single plane linear array of 128 piezoelectric transducers is used for the transmission and the reception. The array pitch is 0.5 mm and the central frequency is 1.5 MHz with 60% bandwidth. This half-wavelength pitch allows a very good spatial sampling of the ultrasonic field.

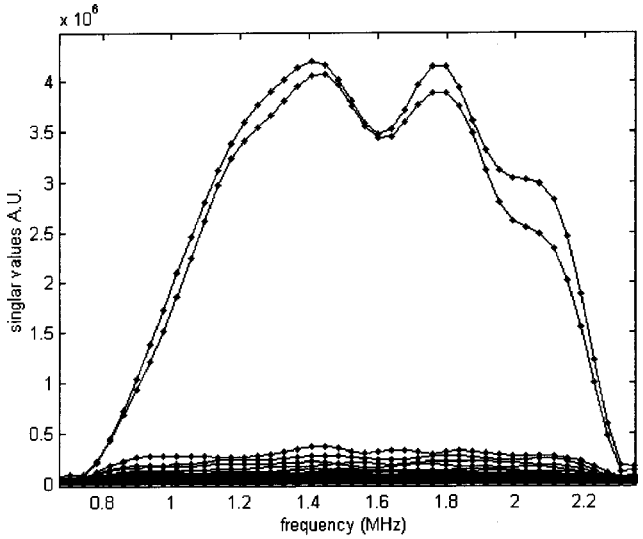

FIG. 2. Singular values versus frequency for a wire separation distance $d=3.5$ mm (arbitrary units).

The height of the piezoelectric transducer is 10 mm. The received signals are sampled at a frequency of 20 MHz. The scatterers are two copper wires of 0.1 mm diameter, which is approximately a tenth of a wavelength. The wires are placed perpendicular to the array at a range of 60 mm. They can be considered as point-like in the plane of insonification. This setting and the small size of the scatterers ensures a Rayleigh-like scattering for the whole bandwidth of the transducers. A translation system was built to vary precisely the distance between the wires. The two wires are stretched on a rigid frame. The fasteners of one of them are mobile on slides and the distance between the wires is then regulated with block gauges.

A. Acquisition of the array response matrix

The most natural way to acquire the array response matrix is to use the canonical basis, that is to say, to acquire separately the response of each pair of elements in the array. However, in our experiment the scattered energy is weak as each scatterer is small compared to the wavelength. In order to improve the signal to noise ratio, the array was driven using the more energetic Walsh function basis,[17] an orthonormal basis in which all the elements are excited in each transmission. However, the measured matrix is transformed to the canonical basis before computing its SVD. This procedure allows a significant increase of signal to noise ratio (around 20 dB for an array of 128 elements). Acquisition of the array response matrix was done for several wire separation distances **d** ranging from 0.3 to 3.5 mm.

B. Result of the decomposition for well-resolved scatterers $d=3.5$ mm

In the case of two targets separated by a distance much greater than the array point spread function, the corresponding Green's functions are almost orthogonal. The SVD of the matrix **K** provides a decomposition of the received signal space into a signal subspace of rank 2 and a noise subspace of rank 126. Figure 2 displays the amplitude of the singular values for all frequencies in the bandwidth of the transducers. As the two wires are identical and well resolved, the two

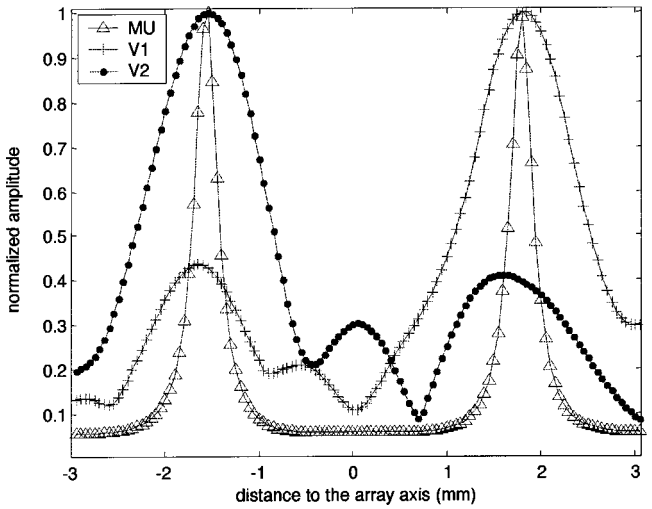

FIG. 3. Wires spaced 3.5 mm, image obtained by back-propagation of the two main eigenvectors (V1 and V2), compared to the image obtained by MUSIC at frequency 1.52 MHz.

highest singular values have almost the same amplitude. To locate the two scatterers, one may compute the scalar product of the singular vectors V_1 and V_2 with the Green's function $G(M)$ for all points M in the area of interest. This treatment is a focusing in receive mode also called back-propagation or virtual time reversal. This treatment in receive mode provides the position of each scatterer (Fig. 3, ● and +). In this case, each singular vector focuses onto both scatterers. In fact, even if the two scatterers are well resolved by the array, the symmetry of the experiment causes a significant coupling between the scatterers' responses that has a strong influence on the singular vectors. In several papers, we have used this back-propagation to make different images with the dominant singular vectors.[1–5]

Using the MUSIC estimator, a higher resolution is achieved. The main lobes of the image provided by MUSIC is five times thinner than with conventional focusing. However, the evaluation of the resolution limit of these methods can only be achieved by studying less distant scatterers. This will be pursued in Sec. V D.

C. The singular values as a function of the distance between the scatterers

When the distance between the two wires decreases to zero, the correlation between the two corresponding Green's functions increases. This coupling modifies the singular values. In the present case of two identical scatterers of reflectivity C in a symmetrical geometry, the first two singular values can be expressed:

$$s_{\pm}=C\left(\sum_{l=1}^{N}|H_{1l}|^2\pm\sum_{l=1}^{N}H_{1l}H_{2l}^{*}\right). \tag{18}$$

We see that if the two scatterers are very close, $H_1\approx H_2=H$ and $H_1-H_2=dH$, and Eq. (18) can be approximated by

$$s_{+}=2C\|H\|^2 \quad \text{and} \quad s_{-}=2C\langle H|dH\rangle.$$

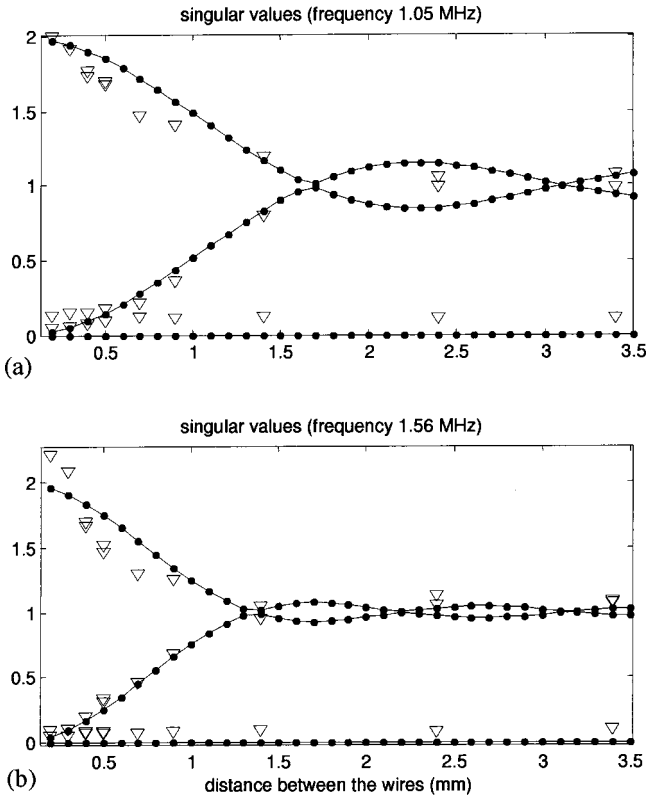

FIG. 4. Experimental (triangle) three main singular values versus the wire separation distance compared with a model (solid line with full circle); (a) frequency 1.05 MHz and (b) frequency 1.56 MHz.

When the scatterers get closer, s_{+} converges to twice the apparent reflectivity of the scatterers, while s_{-} converges toward 0.

A simple model using $\exp(jkr)/\sqrt{r}$ as a surrogate for the 2-D free space Green's function, and the assumption that the transducers are point-like was used to calculate the theoretical singular values of the array response matrix. These theoretical values are compared to the experimental ones in Fig. 4.

The third experimental singular value shows the noise level. It appears to be independent of the distances between the wires. We see that when the distance between the wires reaches 0.4 mm (or 0.4 wavelengths) the second singular value reaches the noise singular values. Looking only at the singular values, one may conclude that wires closer than half a wavelength cannot be distinguished. However, as will be shown later, higher resolution can be achieved through appropriate processing in reception.

Furthermore, for distances between the wires smaller than the wavelength, there is some discrepancy between the theoretical and experimental singular values. Introducing multiple scattering in the simulation, a similar effect is observed on the first singular value (Fig. 5). It is interesting to note that multiple scattering does not change the number of significant singular values. Though multiple scattering induces a global phase shift and global amplitude factor on the wave front emerging from the two wires, the wave impinging on array elements is still a linear combination of these two

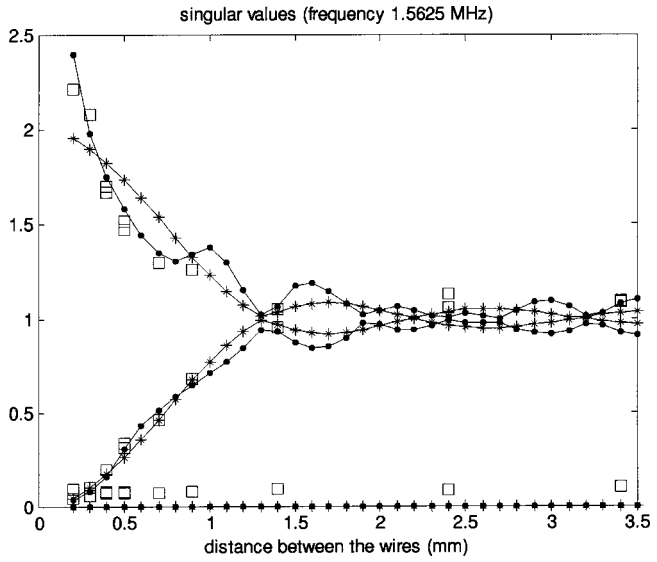

FIG. 5. Three main singular values versus the wire separation distance compared with a model, taking into account multiple scattering at frequency 1.56 MHz. Experiment: square symbol, simple model: solid line with stars, model taking into account multiple scattering: solid line with dots.

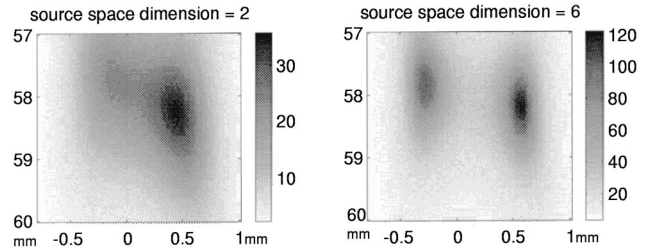

FIG. 6. Image obtained with the MUSIC criterion assuming a signal space of dimension 2 (left) and of dimension 6 (right).

wave fronts, consequently, the rank of the matrix **K** is unchanged.

D. Detection and localization for subwavelength separation

The following experimental results demonstrate the super resolution property of the Maximum Likelihood and MUSIC methods in the case of active array and scatterers. The analysis is performed for frequencies between 0.8 and

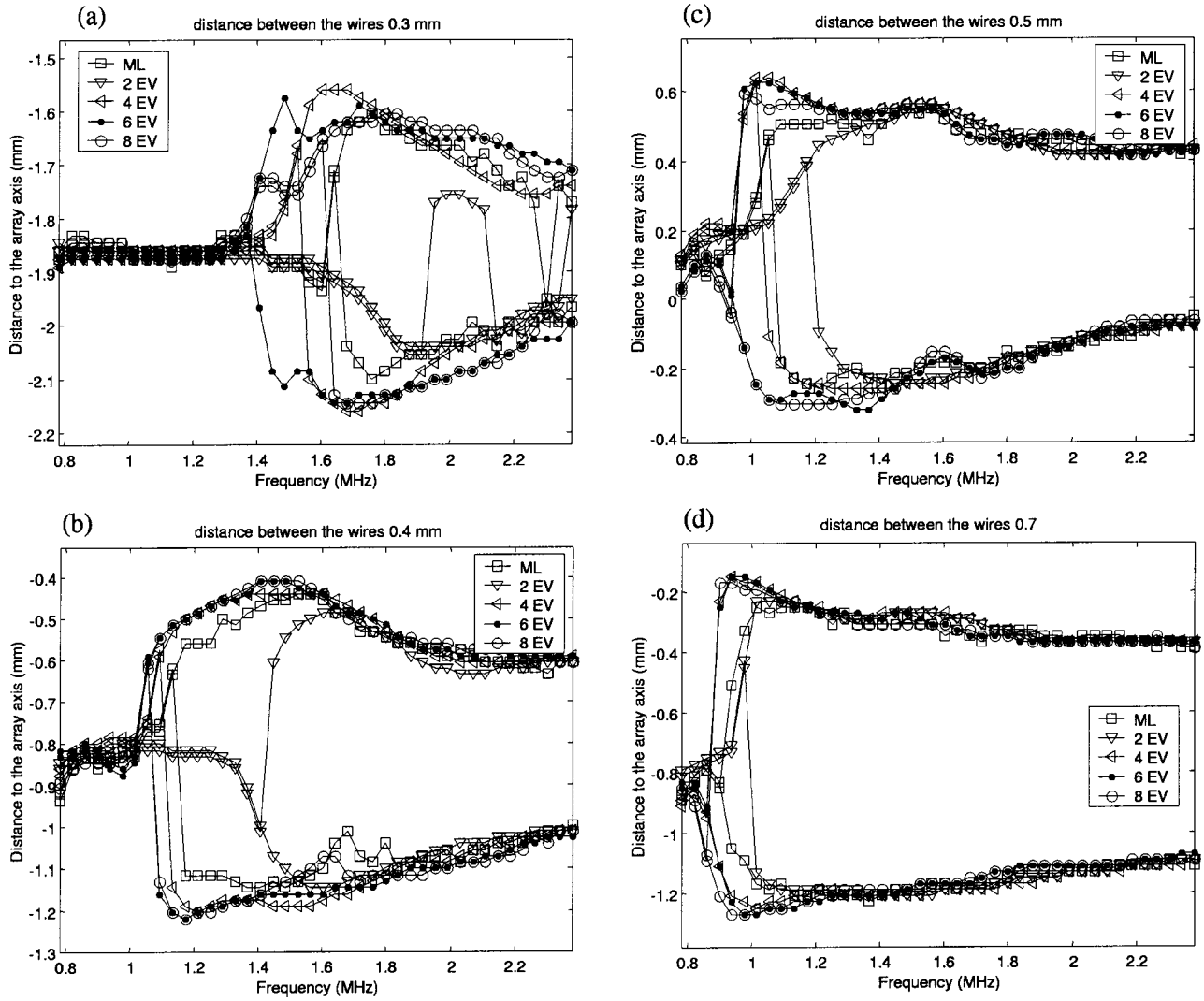

FIG. 7. Estimated lateral coordinates for the Maximum Likelihood (ML) and for the MUSIC algorithm assuming the signal space has dimension 2, 4, 6, and 8 (2, 4, 6, and 8 eV). From top to bottom the distances between the wires are 0.3, 0.4, 0.5, and 0.7 mm.

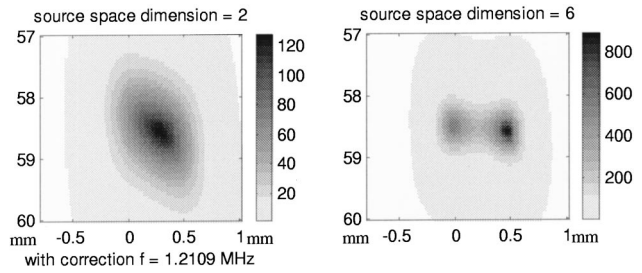

FIG. 8. Image obtained with MUSIC criterion for a signal space of dimension 2 (left) and of dimension 6 (right).

2.4 MHz (λ ranging from 0.6 to 1.9 mm) and for wire axis separation distances $d=0.3$, 0.4, 0.5, and 0.7 mm.

The first example examines the case of $d=0.5$ mm. The MUSIC estimator is computed in a small area around the location of the wires at frequency 1.34 MHz and assuming a signal subspace of dimension 2, Fig. 6 left. The image presents two maxima located around 58 mm in range and separated by a distance of around 0.6 mm. The criterion is then computed using the six dominant singular vectors, Fig. 6 right. A significant resolution gain can be observed. This result suggests that the signal subspace has a dimension higher than 2, as predicted by Chambers;[11] more evidence of this is presented later.

To get better estimates of the resolution limit of the MUSIC and ML methods, this processing was repeated for all frequencies and for the four wire separation distances. Furthermore, the MUSIC criterion was computed for a signal subspace of dimension 2, 4, 6, or 8. Figure 7 presents the lateral positions of the maxima for each estimator. This last figure illustrates the super-resolution property of these methods. The best results are obtained with MUSIC for a signal subspace of dimension 6. The resolution frequency threshold is 1.5, 1.1, 1, and 0.9 MHz for expected distances between the wires of 0.3, 0.4, 0.5, and 0.7 mm, respectively. As expected, MUSIC and ML provide much better resolution than classical focusing, for which the point spread function of the array is 1 mm at 1.5 MHz. Furthermore, the resolution limit computed as the ratio between the wavelength and the wire separation distance is, respectively, 3.3, 3.4, 3 and 2.4. For $d=0.5$ mm and $d=0.7$ mm, this resolution threshold is limited primarily by the bandwidth of the transducer. Indeed, the sensitivity below 1 MHz is very weak so that the difference between the second singular value and the noise singular values is small (Fig. 2). For $d=0.3$ mm and $d=0.4$ mm, the separation occurs when the two wires are separated by less than $\lambda/3$. This result is remarkable, as the array is located about 60 wavelengths from the scatterers, where evanescent waves are negligible.

The sharpening of the criterion shown in Fig. 6 and the fact that the best resolution is reached with a signal subspace of dimension 6 (Fig. 7), indicate that each scatterer is associated with a 3-D signal space, as predicted by Chambers[11] in a 2-D configuration. These three dimensions come from the fact that, in general, the incident field is scattered by heterogenities in both density and compressibility. Heterogeneity in compressibility gives rise to monopolar radiation that leads to a lone isotropic singular vector. In contrast, heterogeneity

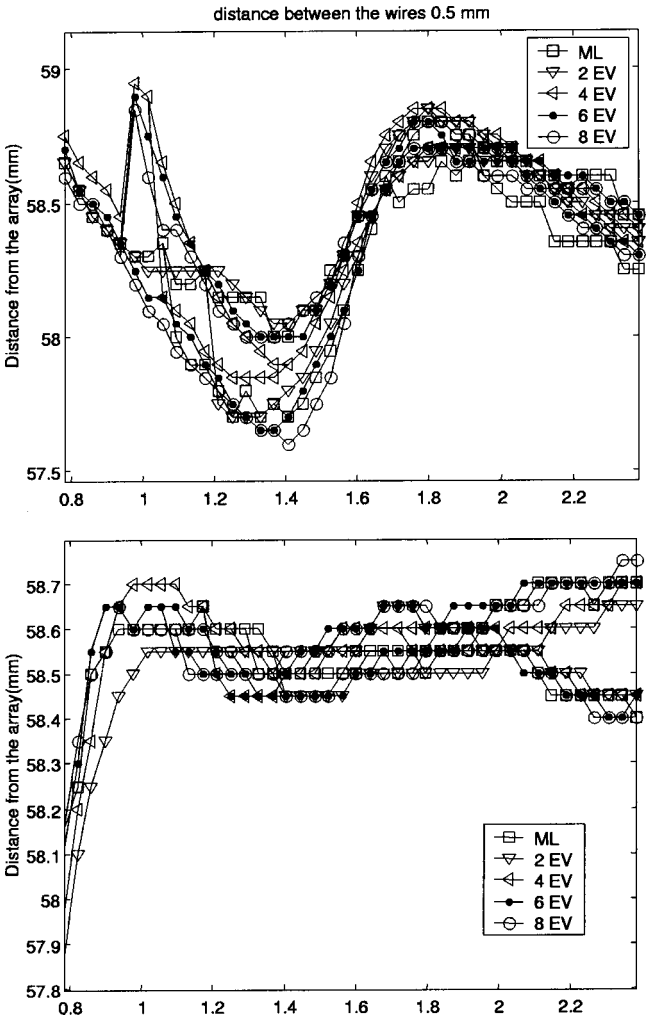

FIG. 9. Distance from the wires to the array (top: no correction; bottom: corrected matrix).

of density gives rise to dipolar radiation. This nonisotropic behavior is responsible for additional singular vectors. This is the first experimental evidence of the existence of these additional singular values.

E. Improvement of the accuracy by correction of the transfer matrix

One important drawback of these two super-resolution methods is the loss of accuracy in the estimated location of the scatterers when the wavelength increases, i.e., the correlation between the responses of the two scatterers increases. This deterioration of the performance is partly accounted for by increased sensitivity to the discrepancies between the true response of each scatterer and the model used. Previously, the array elements were assumed point-like and identical. The model has two main imperfections: first, the sensitivity varies from one element to the other; second, the finite size of the array elements leads to averaging of the incident field and induces amplitude and phase modulation that vary with both the frequency and direction of scattering In the following an empirical correction is applied on the experimental measurements to take into account these array imperfections. As a correction we use the first eigenvector V of the matrix

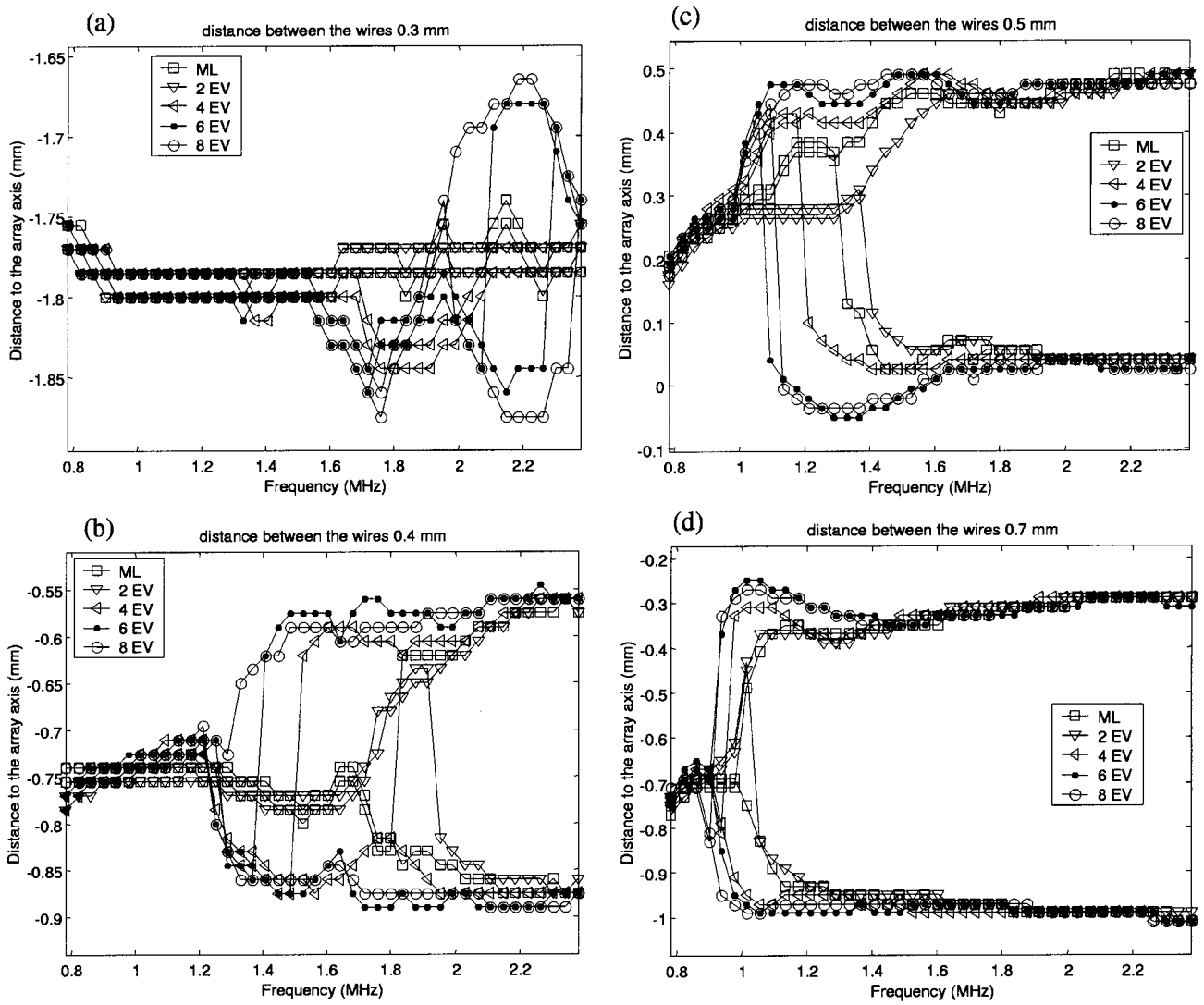

FIG. 10. Estimated coordinate for the corrected matrix using maximum likelihood (ML) and the MUSIC algorithm, assuming the signal space is dimension 2, 4, 6, and 8 (2, 4, 6, and 8 eV). From top to bottom the distances between the wires are 0.3, 0.4, 0.5, and 0.7 mm.

measured for a single wire. The error between this eigenvector and the estimated response Ve is used to compensate each column of the array response matrix $K(\omega)$. More precisely, we replace $K_{ij}(\omega)$ by $K_{ij}(\omega)/V_i(\omega)^* Ve_i(\omega)$, for all pairs i,j. The SVD of the corrected matrix is performed and, as was done to the original matrix, the MUSIC estimator is calculated for signal spaces of dimensions 2 and 6 (Fig. 8). The level of the peak is 7 times higher than before correction (Fig. 6) and the resolution of the image is much better. The improvement is also significant for range localization, as can be seen in Fig. 9. The estimated range is 58.6 mm with a fluctuation of ± 0.15 mm within the whole bandwidth. Without correction, the amplitude fluctuation was larger by at least a factor of 3. Similarly, fluctuations in lateral position are decreased significantly, and now vary by ± 0.025 mm around the mean position (Fig. 10). This is a quarter of the wire diameter.

Our correction, however, decreases the resolution power. The two wires 0.3 mm away are no longer resolved and the resolution threshold is, respectively, 1.4, 1.1, and 0.9 MHz for expected distances between the wires of 0.4, 0.5, and 0.7 mm, respectively. The ratio of wavelength to wire separation is, respectively, 2.7, 2.7, and 2.4. Again the bandwidth is the limiting factor at 0.9 MHz. The experimental Green's function, used to correct our model is necessarily noisy. This produces noise in our empirical model and we believe is responsible for this loss of resolution.

VI. CONCLUSION

In this paper we establish the analogy between the time reversal operator and the pseudocovariance matrix used in high resolution subspace techniques for source detection and localization with passive sensor arrays. As a consequence, the D.O.R.T. method appears as a generalization to active arrays of classical source separation processing. The D.O.R.T. processing starts with the successive transmission of N independent signals resulting in N backscattered wave fronts from which the ''pseudocovariance matrix'' is constructed. The decorrelation of the scatterers' responses is obtained thanks to the spatial diversity of emissions achieved by the array.

An experiment conducted with a linear array of 128 antennas and 2 thin wires illustrates the resolution power of the technique in the farfield. Two estimators were used to determine the position of the wires: the MUSIC and the Maximum Likelihood estimators. Both methods provide resolution much finer than the point spread function, and the best resolution was achieved with the MUSIC algorithm assuming a signal space of dimension 6. The found resolution limit is $\lambda/3$, which is three times smaller than the point spread function (here λ) and beyond the classical diffraction limit $\lambda/2$. For such small distances multiple scattering becomes significant, and we observed that although this phenomenon modifies the eigenvalues distribution, it does not affect the localization process.

The D.O.R.T. method as the time reversal process is robust in heterogeneous media. However, when the acoustic properties of the medium are not constant, any estimator in reception like MUSIC or ML requires an accurate model of the medium. This new method has many potential applications in ultrasonic imaging such as, for example, the detection and localization of flaws in nondestructive evaluation and the detection of mines in underwater acoustics.

[1] C. Prada and M. Fink, ''Eigenmodes of the time reversal operator: a solution to selective focusing in multiple-target media,'' Wave Motion **20**, 151–163 (1994).

[2] C. Prada, J.-L. Thomas, and M. Fink, ''The iterative time reversal process: analysis of the convergence,'' J. Acoust. Soc. Am. **97**, 62–71 (1995).

[3] C. Prada, S. Manneville, D. Spoliansky, and M. Fink, ''Decomposition of the time reversal operator: Application to detection and selective focusing on two scatterers,'' J. Acoust. Soc. Am. **99**, 2067–2076 (1996).

[4] C. Prada, M. Tanter, and M. Fink, ''Flaw detection in solid with the D.O.R.T. method,'' IEEE Ultrason. Symp. Proc. **1**, 681–686 (1997).

[5] E. Kerbrat, C. Prada, D. Cassereau, R. K. Ing, and M. Fink, ''Detection and imaging in complex media with the D.O.R.T. method,'' IEEE Ultrason. Symp. Proc. **1**, 779–783 (2000).

[6] N. Mordant, C. Prada, and M. Fink, ''Highly resolved detection and selective focusing in a waveguide using the D.O.R.T. method,'' J. Acoust. Soc. Am. **105**, 2634–2642 (1999).

[7] T. Yokoyama, T. Kikuchi, T. Tsuchiya, and A. Hasegawa, ''Detection and selective focusing on scatterers using decomposition of time reversal operator method in pekeris waveguide model,'' Jpn. J. Appl. Phys. **40**, 3822–3828 (2001).

[8] H. Tortel, G. Micolau, and M. Saillard, ''Decomposition of the time reversal operator for electromagnetic scattering,'' J. Electromagn. Waves Appl. **13**, 687–719 (1999).

[9] G. Bienvenu and L. Kopp, ''Optimality of high resolution array processing using the eigensystem approach,'' IEEE Trans. Acoust., Speech, Signal Process. **31**, 1235–1247 (1983).

[10] R. O. Schmidt, ''Multiple emitter location and signal parameter estimation,'' IEEE Trans. Antennas Propag. **34**, 276–280 (1989).

[11] D. H. Chambers and A. K. Gautesen, ''Time reversal for a single spherical scatterer,'' J. Acoust. Soc. Am. **109**, 2616–2624 (2001).

[12] S. Komilikis, C. Prada, and M. Fink, ''Characterization of extended objects with the D.O.R.T. method,'' IEEE Ultrason. Symp. Proc. **2**, 1401–1404 (1996).

[13] M. I. Skolnik, RADAR Handbook (McGraw-Hill, New York, 1990).

[14] A. B. Baggeroer, W. A. Kuperman, and P. N. Mikhalevsky, ''An overview of matched Field Methods in Ocean Acoustics,'' IEEE J. Ocean. Eng. **18**, 401–424 (1993).

[15] A. J. Devaney, ''Computational time reversal and object localization'' J. Acoust. Soc. Am **110**, 2617 (2001); or A. J. Devaney, ''Super-resolution processing of multi-static data using time reversal and music,'' submitted to J. Acoust. Soc. Am.

[16] M. Cheney, ''The linear Sampling Method and the MUSIC Algorithm,'' Inverse Probl. **17**, 591–595 (2001).

[17] S. Azzaretti, D. Dotti, R. Lombardi, and D. Rossi, ''Echo-graphic images enhanced through Walsh functions,'' IEEE Ultrason. Symp. Proc. **1**, 675–678 (1997).